J|A|C|S
ARTICLES
Published on Web 01/29/2005

Correlations between ^{31}P Chemical Shift Anisotropy and Molecular Structure in Polycrystalline *O,O′*-Dialkyldithiophosphate Zinc(II) and Nickel(II) Complexes: ^{31}P CP/MAS NMR and Ab Initio Quantum Mechanical Calculation Studies

Anna-Carin Larsson,[†] Alexander V. Ivanov,[‡] Willis Forsling,[†] Oleg N. Antzutkin,*[,†] Anu E. Abraham,[§] and Angel C. de Dios[§]

Contribution from the Division of Chemistry, Luleå University of Technology, S-971 87 Luleå, Sweden, Amur Integrated Research Institute, Far Eastern Branch of the Russian Academy of Sciences, 675000, Blagoveschensk, Amur Region, Russia, and Department of Chemistry, Georgetown University, 37th and O Streets NW, Washington, D.C. 20057

Received November 3, 2003; E-mail: Oleg.Antzutkin@ltu.se

Abstract: Different potassium salts and zinc(II) and nickel(II) *O,O′*-dialkyldithiophosphate complexes were studied by solid-state ^{31}P CP/MAS and static NMR and ab initio quantum mechanical calculations. Spectra were obtained at different spinning frequencies, and the intensities of the spinning sidebands were used to estimate the chemical shift anisotropy parameters. Useful correlations between the shapes of the ^{31}P chemical shift tensor and the type of ligand were found: terminal ligands have negative values of the skew κ, while bridging and ionic ligands have positive values for this parameter. The experimental results were compared with known X-ray diffraction structures for some of these complexes as well as with ab initio quantum mechanical calculations, and a useful correlation between the δ_{22} component of the ^{31}P chemical shift tensor and the S−P−S bond angle in the *O,O′*-dialkyldithiophoshate zinc(II) and nickel(II) complexes was found: δ_{22} increases more than 50 ppm with the increase of S−P−S bond angle from ca. 100° to 120°, while the other two principal values of the tensor, δ_{11} and δ_{33}, are almost conserved. This eventually leads to the change in sign for κ in the bridging type of ligand, which generally has a larger S−P−S bond angle than the terminally bound *O,O′*-dialkyldithiophoshate group forming chelating four-membered P⟨$^{S}_{S}$⟩Me heterocycles.

1. Introduction

Dialkyldithiophosphates are frequently used as analytical reagents for extraction and spectrophotometric determination of metal ions[1a] and as selective flotation agents,[1b] and therefore studies of different *O,O′*-dialkyldithiophosphate metal complexes in the solid state can be of interest. These systems adopt a variety of molecular and crystal structures, mono-, bi-, tetra-, and polynuclear, as have been established previously by means of single-crystal X-ray diffraction analysis.[2] For example, the nickel(II) complexes, [Ni{$S_2P(OR)_2$}$_2$], are mononuclear and contain only terminal chelating ligands.[2a−c] The zinc(II) diethyldithiophosphate complex, [Zn{$S_2P(OC_2H_5)_2$}$_2$]$_\infty$, is crystallized in the form of a long polymeric chain with alternating bridging and terminal ligands.[2d] The other zinc(II) complexes, [Zn_2{$S_2P(OR)_2$}$_4$], are binuclear and contain pairs of both terminal and bridging types of ligands.[2e,f] There are also known tetranuclear zinc(II) dialkyldithiophosphate complexes, [Zn_4X{$S_2P(OR)_2$}$_6$] (X = O, S), with all six ligands of the bridging type and with a central sulfur or oxygen atom tetrahedrally coordinated to four zinc atoms.[2g,h] These four types of molecular structures are schematically shown in Figure 1. Some important crystallographic data for the dialkyldithiophosphate compounds in this study are given in Table 1.

In a previous study of different binuclear and tetranuclear dialkyldithiophosphate zinc(II) complexes in solid and liquid states, and in chloroform solutions, we have assigned the highly shielded ^{31}P CP/MAS NMR resonances of different dithiophosphate zinc(II) complexes to the terminal chelating ligands and the least shielded resonances to the bridging ligands.[2f] On the basis of these results, we also suggested a bridging coordination mode for dialkyldithiophosphates chemisorbed on the surface of synthetic sphalerite, ZnS.[2f] However, for some dithiophos-

[†] Luleå University of Technology.
[‡] Russian Academy of Sciences.
[§] Georgetown University.

(1) (a) Stary, J. *The Solvent Extraction of Metal Complexes*; Pergamon Press: New York, 1964. (b) Kabovski, A. *Proceedings of the International Congress on Surface Activity, II*; London, 1955; p 222.
(2) (a) McConnell, J. F.; Kastalsky, V. *Acta Crystallogr.* **1967**, *22*, 853. (b) Ivanov, A. V.; Larsson, A.-C.; Rodionova, N. A.; Gerasimenko, A. V.; Antzutkin, O. N.; Forsling, W. F. *Russ. J. Inorg. Chem. (Engl. Transl.)* **2004**, *49*, 373. (c) Hoskins, B. F.; Tiekink, E. R. T. *Acta Crystallogr.* **1985**, *C41*, 322. (d) Ito, T.; Igarashi, T.; Hagihara, H. *Acta Crystallogr.* **1969**, *B25*, 2303. (e) Lawton, S. L.; Kokotailo, G. T. *Inorg. Chem.* **1969**, *8*, 2410. (f) Ivanov, A. V.; Antzutkin, O. N.; Larsson, A.-C.; Kritikos, M.; Forsling, W. *Inorg. Chim. Acta* **2001**, *315*, 26. (g) Harrison, Ph. G.; Begley, M. J.; Kikabhai, T.; Killer, F. *J. Chem. Soc., Dalton Trans*. **1986**, 925. (h) Burn, J.; Smith, G. W. *Chem. Commun.* **1965**, 394.

10.1021/ja0306112 CCC: $30.25

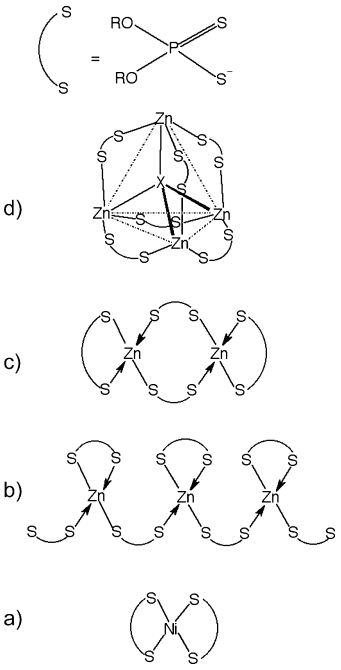

Figure 1. Schematic representation of the molecular structures of nickel(II) *O*,*O*′-dialkyldithiophosphate (a), polymeric zinc(II) *O*,*O*′-diethyldithiophosphate (b), binuclear zinc(II) *O*,*O*′-dialkyldithiophosphate (c), and tetranuclear zinc(II) *O*,*O*-dialkyldithiophosphate (d) complexes.

phate ligands adsorbed on the sphalerite surface, ^{31}P NMR spectra showed rather broad (>3 ppm) resonance lines that cover the whole range of isotropic chemical shifts for both terminal and bridging ligands of the polycrystalline zinc dithiophosphate complexes. To resolve the issue of assignment of chemisorbed species, we address the possibility of using the full ^{31}P chemical shift tensor (CST) rather than the isotropic chemical shifts alone.

For powders, only the three principal values of the CST, and not the orientation, can be determined if no other tensorial interactions, such as dipole−dipole coupling, with a known orientation in the molecular frame, also contribute to the NMR spectrum. Nevertheless, knowledge of the principal values of the CSTs alone is useful for structural analysis. The principal values, δ_{11}, δ_{22}, and δ_{33}, can be derived from the singularities in the shape of a static spectrum.[3] However, for static solid-state NMR, the resolution is low and the principal values cannot be determined accurately since the edges of the powder pattern are often distorted. It might even be impossible to distinguish these singularities if there are several powder patterns superimposed in the spectrum. At magic-angle spinning, the spectrum consists of sharp central bands at the isotropic chemical shifts winged by spinning sidebands at positions of $n\omega_r$ ($n = \pm1, \pm2,$ ...) from the central band, where ω_r is the spinning frequency. Herzfeld and Berger have shown that the intensities of the spinning sidebands can be used to accurately estimate the three principal values of the CST.[4a] A comparative study between static and spinning spectra shows that the reliability in the determination of the chemical shift anisotropy (CSA) parameters is better for slow magic-angle spinning than for static NMR spectra if the number of spinning sidebands dominating in the spectral pattern is more than 8.[4b] Levitt and co-workers have developed a robust and convenient program in the Mathematica front end for the CSA analysis of MAS NMR spectra using intensities of up to ±11 spinning sidebands.[5]

In this study we analyze the ^{31}P CSA of the dialkyldithiophosphate compounds, whose isotropic chemical shifts were studied earlier,[2f] by evaluating the intensities of the spinning sidebands in the CP/MAS NMR spectra obtained at moderate and slow sample spinning. The analysis was performed using the program developed by Levitt and co-workers.[5]

To understand further the observed trends for ^{31}P shielding tensors in the dialkyldithiophosphates, ab initio quantum mechanical calculations of the shielding tensor were also performed. It is hoped that these computations will illustrate how useful ab initio studies are in interpreting solid-state NMR data. The quality of shielding computational methodologies has already approached the accuracy of experimental results, at least for first-row elements.[6] Two sets of calculations are presented. The first one involved a systematic study of how the internal geometry coordinates relevant to the phosphorus sites influence the principal components of the shielding tensor. These calculations were performed on a small molecular model fragment. It was hoped that through this strategy, the factor responsible for the experimental trends seen could be correctly identified. The second set made use of optimized geometries for the compounds whose shielding tensors were experimentally measured and presented in this paper. This set provided a gauge of how accurate geometry optimizations and shielding computations presently are for this specific set of dithiophosphates.

The ^{31}P chemical shielding tensors in a number of different phosphates, phosphate esters, phospholipids, phosphides, and phosphindisulfides have been previously studied, both experimentally and theoretically.[7a−m] For example, Un and Klein have found empirical linear correlations between P−O bond lengths, O−P−O bond angles (in a number of phosphates and phosphate esters), and the σ_{11} and σ_{33} chemical shielding tensor elements of phosphorus sites that was explained as a result of the extent of d_P-p_O π-character of these bonds and angles.[7a] Potrzebowski has studied bis(organothiophosphoryl)disulfides and also has found linear correlations between P−S bond lengths, S−P−S bond angles, and the ^{31}P CSA parameters for these compounds.[7b] In our work, a similar linear correlation between the S−P−S bond angle and the ^{31}P CST principal value, δ_{22}, of Ni(II) and

(3) (a) Bloembergen, N.; Rowland, J. A. *Acta Metall.* **1953**, *1*, 731. (b) Grant, D. M. In *Encyclopedia of Nuclear Magnetic Resonance*; Grant, D. M., Harris, R. K., Eds.; Wiley: New York, 1996; p 1298.
(4) (a) Herzfeld, J.; Berger, A. E. *J. Chem. Phys.* **1980**, *73*, 6021. (b) Hodgkinson, P.; Emsley, L. *J. Chem. Phys.* **1997**, *107*, 4808.
(5) Antzutkin, O. N.; Lee, Y. K.; Levitt, M. H. *J. Magn. Reson.* **1998**, *135*, 144.
(6) Rich, J. E.; Manalo, M. N.; de Dios, A. C. *J. Phys. Chem. A* **2000**, *104*, 5837.
(7) (a) Un, S.; Klein, M. P. *J. Am. Chem. Soc.* **1989**, *111*, 5119. (b) Potrzebowski, M. J. *J. Chem. Soc., Perkin. Trans.* **1993**, 63. (c) Hauser, H.; Radloff, C.; Ernst, R. R.; Sundell, S.; Pascher, I. *J. Am. Chem. Soc.* **1988**, *110*, 1054. (d) Bechmann, M.; Dusold, S.; Forster, H.; Haeberlen, L.; Lis, T.; Sebald, A.; Stumber, M. *Mol. Phys.* **2000**, *98*, 605. (e) Alam, T. M. *Int. J. Mol. Sci.* **2002**, *3*, 8. (f) Bernard, G. M.; Wu, G.; Lumsden, M. D.; Wasylishen, R. E.; Maigrot, N.; Charrier, C.; Mathey, F. *J. Phys. Chem. A* **1999**, *103*, 1029. (g) Fleischer, U.; Frick, F.; Grimmer, A. R.; Hoffbauer, W.; Jansen, M.; Kutzelnigg, W. *Z. Anorg. Allg. Chem.* **1995**, *621*, 2012. (h) Gibby, M. G.; Pines, A.; Rhim, W.-K.; Waugh, J. S. *J. Chem. Phys.* **1972**, *56*, 991. (i) Tullius, M.; Lathrop, D.; Eckert, H. *J. Phys. Chem.* **1990**, *94*, 2145. (j) Woo, A. J.; Kim, S.-J.; Park, Y. S.; Goh, E.-Y. *Chem. Mater.* **2002**, *14*, 518. (k) Potrzebowski, M. J.; Assfeld, X.; Ganicz, K.; Olejniczak, S.; Cartier, A.; Gardiennet, C.; Tekely, P. *J. Am. Chem. Soc.* **2003**, *125*, 4223. (l) Eichele, K.; Wasylishen, R. E.; Corrigan, J. F.; Taylor, N. J.; Carty, A. J.; Feindel, K. W.; Bernard, G. M. *J. Am. Chem. Soc.* **2002**, *124*, 1541. (m) Gee, M.; Wasylishen, R. E.; Eichele, K.; Britten, J. F. *J. Phys. Chem. A* **2000**, *104*, 4598.

Table 1. Crystallographic Data for *O,O′*-Dialkyldithiophosphate Complexes

complex	P–O (Å)	P–S (Å)	S–P–S (°)	O–P–O (°)
$[Ni\{S_2P(OC_2H_5)_2\}_2]^a$	1.579 ± 0.009	1.986 ± 0.006	103.1 ± 0.2	96.6 ± 0.5
	1.571 ± 0.009	1.993 ± 0.005		
	mean 1.575	mean 1.990		
$[Ni\{S_2P(OC_3H_7)_2\}_2]^b$ *	1.5656 ± 0.0009	2.0037 ± 0.0006	102.09 ± 0.02	96.80 ± 0.05
	1.569 ± 0.001	1.9966 ± 0.0006		
	1.568 ± 0.001	2.0022 ± 0.0006	102.02 ± 0.02	96.99 ± 0.05
	1.5705 ± 0.0009	2.0046 ± 0.0006		
	mean 1.568	mean 2.0018	mean 102.06	mean 96.90
$[Ni\{S_2P(O\text{-}i\text{-}C_3H_7)_2\}_2]^c$	1.564 ± 0.003	1.991 ± 0.002	101.7 ± 0.1	96.9 ± 0.2
	1.566 ± 0.003	1.993 ± 0.001		
	mean 1.565	mean 1.992		
α-$[Ni\{S_2P(O\text{-}i\text{-}C_4H_9)_2\}_2]^b$ *	1.561 ± 0.003	1.985 ± 0.002	102.78 ± 0.06	96.7 ± 0.2
T < 296 K	1.565 ± 0.003	1.992 ± 0.002		
	1.562 ± 0.003	1.989 ± 0.002	102.91 ± 0.07	96.2 ± 0.2
	1.565 ± 0.003	1.988 ± 0.002		
	mean 1.563	mean 1.988	mean 102.84	mean 96.4
$[Zn\{S_2P(OC_2H_5)_2\}_2]_n^d$	1.57 ± 0.01 (B)**	1.992 ± 0.007 (B)	108.0 ± 0.3 (B)	97.4 ± 0.7 (B)
	1.57 ± 0.01 (B)	2.001 ± 0.005 (B)		
	mean 1.57	mean 1.996		
	1.56 ± 0.02 (T)**	1.987 ± 0.009 (T)	109.7 ± 0.4 (T)	94.5 ± 1.2 (T)
	1.62 ± 0.02 (T)	1.973 ± 0.011 (T)		
	mean 1.59	mean 1.980		
$[Zn_2\{S_2P(O\text{-}i\text{-}C_3H_7)_2\}_4]^e$	1.60 ± 0.01 (B)	1.957 ± 0.007 (B)	117.3 ± 0.3 (B)	104.4 ± 0.8 (B)
	1.58 ± 0.02 (B)	1.971 ± 0.007 (B)		
	mean 1.59	mean 1.964		
	1.56 ± 0.01 (T)	1.984 ± 0.007 (T)	109.7 ± 0.3 (T)	94.9 ± 0.8 (T)
	1.57 ± 0.01 (T)	1.968 ± 0.007 (T)		
	mean 1.56	mean 1.976		
$[Zn_2\{S_2P(O\text{-}c\text{-}C_6H_{11})_2\}_4]^f$	1.563 ± 0.006 (B)	1.988 ± 0.003 (B)	115.73 ± 0.13 (B)	100.9 ± 0.3 (B)
T < 316 K	1.582 ± 0.005 (B)	1.992 ± 0.003 (B)		
	mean 1.572	mean 1.990		
	1.569 ± 0.005 (T)	1.995 ± 0.003 (T)	109.11 ± 0.12 (T)	96.4 ± 0.3 (T)
	1.571±0.005 (T)	1.992 ± 0.003 (T)		1.992±0.003 (T)
	mean 1.570	mean 1.994		mean 1.994
$[Zn_4S\{S_2P(OC_2H_5)_2\}_6]^g$	1.60 ± 0.01	1.983 ± 0.005	120.5 ± 0.2	101.6 ± 0.5
	1.568 ± 0.09	1.993 ± 0.005	121.1 ± 0.2	100 ± 0.1
	1.53 ± 0.01	1.981 ± 0.006		
	1.56 ± 0.02	1.968 ± 0.006		
	mean 1.56	mean 1.981		

[a] Reference 2a. [b] Reference 2b. [c] Reference 2c. [d] Reference 2d. [e] Reference 2e. [f] Reference 2f. [g] Reference 2g. *****Ni-*n*-Pr-dtp has two centrosymmetric structurally nonequivalent molecules, while Ni-*i*-Bu-dtp exists as a unique molecule including two structurally nonequivalent ligands. **(B) = bridging and (T) = terminal ligands.

Zn(II) dialkyldithiophosphate complexes was found in experimental ^{31}P NMR spectra and further supported by ab initio quantum mechanical calculations.

2. Experimental Section

2.1. Materials. Eight different potassium salts of dialkyldithiophosphates (alkyl groups were ethyl, *n*-propyl, *i*-propyl, *n*-butyl, *i*-butyl, *s*-butyl, *i*-amyl, and *cyclo*-hexyl), commercial collectors Danafloat, were provided to us by CHEMINOVA AGRO A/S both as solids and as aqueous solutions.

Mononuclear nickel(II) and binuclear, tetranuclear, and polynuclear zinc(II) *O,O′*-dialkyldithiophosphate complexes were prepared from aqueous solutions of $NiCl_2$ or $ZnCl_2$ and the *O,O′*-dialkyldithiophosphate salts according to previously described methods.[2d,e,g,8,9] Precipitated complexes were filtered off, washed with deionized water, and dried in air without further purification. In cases of structurally disordered systems that showed broad ^{31}P CP/MAS NMR resonance lines, samples were additionally recrystallized from chloroform.

2.2. Physical Measurements. Solid-state ^{31}P magic-angle-spinning (MAS) NMR spectra were recorded on a Varian/Chemagnetics Infinity CMX-360 (B_0 = 8.46 T) spectrometer using cross-polarization (CP) from the protons together with proton decoupling.[10] The ^{31}P operating frequency was 145.73 MHz. The proton $\pi/2$ pulse duration was 5.2 μs, CP mixing time varied between 1 and 3 ms for different samples, and the nutation frequency of protons during decoupling was $\omega_{nut}/2\pi$ = 64 kHz. From 4 to 128 transients spaced by a relaxation delay from 2 to 5 s were accumulated. Powder samples were packed in zirconium dioxide standard double-bearing 7.5 mm rotors. All samples were recorded at two or more different spinning frequencies, between 1 and 6 kHz, and their isotropic chemical shift data (in the deshielding, δ-scale) are given with respect to 85.5% H_3PO_4[11] (here 0 ppm, externally referenced) that was mounted in a short capillary glass tube (diameter 1 mm) and placed in a 7.5 mm rotor to minimize errors due to differences in the magnetic susceptibility (<0.1 ppm).

Static ^{31}P NMR spectra shown in the Supporting Information were obtained with a spin−echo experiment described by Oldfield and coworkers,[12] modified by us to incorporate both cross-polarization from

(8) Drew, M. G. B.; Hasan, M.; Hobson, R. J.; Rice, D. A. *J. Chem. Soc., Dalton Trans*. **1986**, 1161.
(9) Wystrach, V. P.; Hook, E. O.; Christopher, G. L. M. *J. Org. Chem*. **1956**, *21*, 705.
(10) Pines, A.; Gibby, M. G.; Waugh, J. S. *J. Chem. Phys*. **1972**, *56*, 1776.
(11) Karaghiosoff, K. In *Encyclopedia of Nuclear Magnetic Resonance*; Grant, D. M., Harris, R. K., Eds.; Wiley: New York, 1996; p 3612.
(12) Kunwar, A. C.; Turner, G. L.; Oldfield, E. *J. Magn. Reson.* **1986**, *69*, 124.

the protons and proton decoupling. In these experiments, the ^{31}P 180° pulse duration was 10 μs, and the echo delay was 100 μs. From 128 to 1024 transients with a relaxation delay of 3 s were accumulated.

2.3. CSA Simulations. Simulations of the ^{31}P CSA parameters were performed in a Mathematica program developed by Levitt and co-workers.[5] The input file to the program consists of the experimental sideband intensities, the experimental spinning frequency, the Larmor frequency, and the experimental noise variance. The program plots the chi-square statistics, χ^2, as a function of the two chemical shift anisotropy parameters δ_{aniso} and η, with a minimum at certain values of δ_{aniso} and η.[13] The joint confidence regions of the two CSA parameters are bounded by the contours $\chi^2 = \chi_{min}^2 + 2.3$ (68.3% joint confidence limit) and $\chi^2 = \chi_{min}^2 + 6.17$ (95.4% joint confidence limit).[14] The principal values of the CST, δ_{11}, δ_{22}, and δ_{33}, were recalculated from δ_{aniso} and η (see Supporting Information).

The sideband intensities were measured with the deconvolution method by using the builtin "Spinsight" spectrometer software. Values of δ_{aniso} and η from simulations at two different spinning frequencies were obtained, and their mean and the mean statistical errors were also calculated (see eq 3 in Supporting Information). A two-tailed *F*-test was performed to confirm that the CSA values obtained from spectra measured at the two different spinning frequencies did not differ significantly from each other.[15] The confidence intervals for the CST principal values were calculated from confidence intervals for δ_{aniso} and η using the partial derivative method (see eq 4 in Supporting Information).[16] For more details concerning the calculations of the CST principal values and their confidence intervals, see the Supporting Information.

2.4. Ab Initio Calculations. Calculations were performed on bis(*O*,*O*′-diethyldithiophosphato-*S*,*S*′)nickel(II) [Ni{$S_2P(OC_2H_5)$}$_2$], bis(*O*,*O*′-di-isopropyldithiophosphato-*S*,*S*′)nickel(II) [Ni{S_2P(O-*i*-C_3H_7)}$_2$], *catena*-poly[(μ_2-*O*,*O*′-diethyldithiophosphato-*S*,*S*′)(*O*,*O*′-diethyldithiophosphato)zinc(II)] [Zn{$S_2P(OC_2H_5)$}$_2$]$_\infty$, bis[μ_2-(*O*,*O*′-di-isopropyldithiophosphato-*S*,*S*′)(*O*,*O*′-di-isopropyldithiophosphato)]dizinc(II) [Zn_2-{S_2P(O-*i*-C_3H_7)}$_4$], and hexakis[μ_2-(*O*,*O*′-diethyldithiophosphato-*S*,*S*′)]-μ_4-thio-tetrazinc [Zn_4S{$S_2P(OC_2H_5)$}$_6$] compounds. The principal components of the shielding tensor were defined as $\sigma_{11} \leq \sigma_{22} \leq \sigma_{33}$. The principal components of the NMR chemical shift tensor, δ_{ii}, are defined such that the two parameters δ_{ii} and σ_{ii} increase in opposite directions, $\delta_{11} \geq \delta_{22} \geq \delta_{33}$, following the notations of Mason.[17] The isotropic shielding and the isotropic chemical shift are simply the arithmetic averages of the principal tensor components. The span (Ω) and the skew (κ) are also useful parameters that can describe the tensor. They are defined by the following equations:[17]

$$\Omega = \sigma_{33} - \sigma_{11} = \delta_{11} - \delta_{33}$$

$$\kappa = 3(\sigma_{iso} - \sigma_{22})/\Omega = 3(\delta_{22} - \delta_{iso})/\Omega$$

The skew, $\kappa = \pm 1$, corresponds to axially symmetric shielding tensors with the asymmetry parameter $\eta = 0$ (a prolate ($\kappa = +1$) or an oblate ($\kappa = -1$) ellipsoids), while $\kappa = 0$ corresponds to the asymmetric shielding tensor with $\eta = 1$.

All computations were performed using a parallel version of Gaussian98.[18] The effects of changes in the bond lengths (P−O and P−S) and in the bond angles (O−P−O and S−P−S) on the ^{31}P shielding tensor were determined using a model molecule, $[(CH_3O)_2PS_2]^-$.

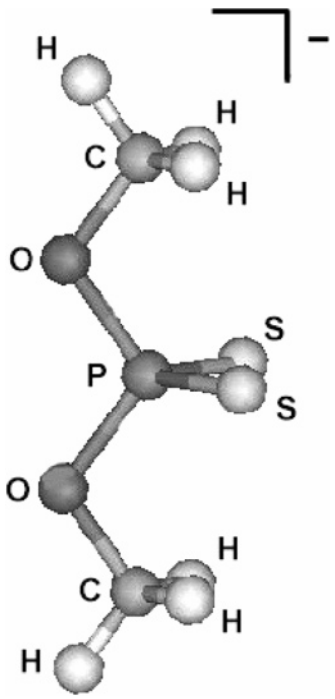

Figure 2. Model $[(CH_3O)_2PS_2]^-$ fragment used in ab initio calculations of the ^{31}P shielding tensor.

Figure 2 shows a cartoon for this model fragment. Principal axes *x*, *y*, and *z* corresponding to the ^{31}P chemical shift tensor elements δ_{11}, δ_{22}, and δ_{33} were found as follows: *z* bisects the S−P−S angle, *y* is perpendicular to the plane formed by S, P, and S atoms, and *x* is perpendicular to both *y* and *z*. The carbon and hydrogen atoms in this model were assigned with the 6-31G basis set, while a 6-31G** basis set was used for the remaining atoms. These shielding calculations were performed at the B3LYP level of theory, a hybrid method that uses the Becke exchange functional[19] mixed with Hartree−Fock contributions and the correlation functional of Lee, Yang, and Parr.[20]

A complete geometry optimization of the single-crystal X-ray diffraction data for the zinc(II) and nickel(II) dialkyldithiophosphate complexes was deemed necessary after observing from calculations the extreme sensitivity of the ^{31}P shielding tensor on the positions of the oxygen and sulfur atoms to which it is bound. These calculations were likewise performed at the B3LYP level of theory, with the 6-31G basis set for carbon and hydrogen atoms and 6-31G** for phosphorus, sulfur, and oxygen. Regardless of its identity, the metal atom in each compound was given a LANL1MB effective core potential. For these large nuclei, the electrons that are near the nucleus are approximated via electron core potentials (ECP). For the [Ni{$S_2P(OC_2H_5)_2$}$_2$] system we also tested a DZ basis set on the nickel atom. However, the effects of the DZ basis on the calculated ^{31}P shielding tensor were found to be much smaller than the effects of the basis set on P, S, and O atoms. The NMR shielding tensors were calculated using the optimized structures

(13) Defined as $\delta_{aniso} = (\delta_{33} - \delta_{iso})$ and $\eta = (\delta_{22} - \delta_{11})/(\delta_{33} - \delta_{iso})$ when $|\delta_{11} - \delta_{iso}| \leq |\delta_{33} - \delta_{iso}|$ or as $\delta_{aniso} = (\delta_{11} - \delta_{iso})$ and $\eta = (\delta_{22} - \delta_{33})/(\delta_{11} - \delta_{iso})$ when $|\delta_{11} - \delta_{iso}| \geq |\delta_{33} - \delta_{iso}|$.

(14) Press, W. H.; Teukolsky, S. A.; Vetterling, W. T.; Flannery, B. P. *Numerical Recipes In C*; Cambridge Univ. Press: Cambridge, UK, 1994; p 697.
(15) Miller, J. C.; Miller, J. N. *Statistics For Analytical Chemistry*, 3rd ed.; Ellis Horwood Ptr/Prentice Hall: New York, 1993; p 60.
(16) Kragten, J. *Analyst* **1994**, *119*, 2161.
(17) Mason, J. *Solid State Nucl. Magn. Reson*. **1993**, *2*, 285.
(18) Frisch, M. J.; Trucks, G. W.; Schlegel, H. B.; Scuseria, G. E.; Robb, M. A.; Cheeseman, J. R.; Zakrzweski, V. G.; Montgomery, J. A., Jr.; Stratmann, R. E.; Burant, J. C.; Dapprich, S.; Millam, J. M.; Daniels, A. D.; Kudin, K. N.; Strain, M. C.; Farkas, O.; Tomasi, J.; Barone, V.; Cossi, M.; Cammi, R.; Mennucci, B.; Pomelli, C.; Damo, C.; Clifford, S.; Ochterski, J.; Petersson, G. A.; Ayala, P. Y.; Cui, Q.; Morokuma, K.; Malick, D. K.; Rabuck, A. D.; Raghavachari, K.; Foresman, J. B.; Cioslowski, J.; Ortiz, J. V.; Baboul, A. G.; Stefanov, B. B.; Liu, G.; Liashenko, A.; Piskorz, P.; Komaromi, I.; Gomperts, R.; Martin, R. L.; Fox, D. J.; Keith, T.; Al-Laham, M. A.; Peng, C. Y.; Nanayakkara, A.; Gonzalez, C.; Challacombe, M.; Gill, P. M. W.; Johnson, B.; Chen, W.; Wong, M. W.; Andres, J. L.; Gonzalez, C.; Head-Gordon, M.; Replogle, E. S.; Pople, J. A. *Gaussian 98*, Revision A.7; Gaussian, Inc.: Pittsburgh, PA, 1998.
(19) Becke, A. D. *J. Chem. Phys.* **1993**, *98*, 5648.
(20) Lee, C.; Yang, W.; Parr, R. G. *Phys. Rev. B* **1988**, *37*, 785.

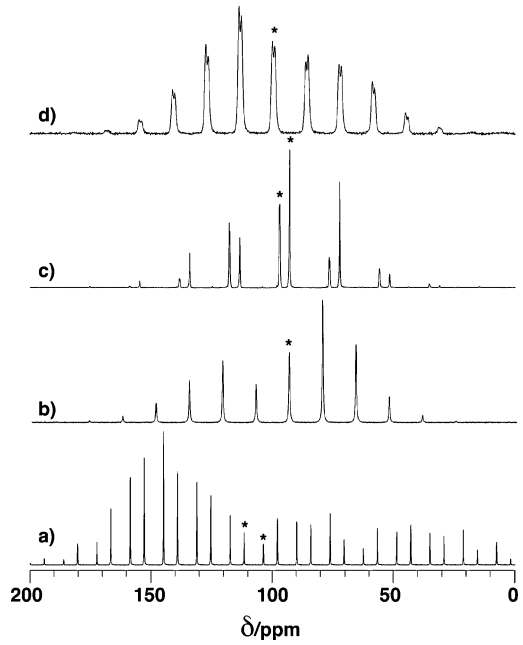

Figure 3. ^{31}P CP/MAS NMR spectra of powder *O*,*O*′-di-isopropyldithiophosphate compounds: potassium salt, $KS_2P(O\text{-}i\text{-}C_3H_7)_2$ (a), mononuclear $[Ni\{S_2P(O\text{-}i\text{-}C_3H_7)_2\}_2]$ (b), binuclear $[Zn_2\{S_2P(O\text{-}i\text{-}C_3H_7)_2\}_4]$ (c), and tetranuclear $[Zn_4O\{S_2P(O\text{-}i\text{-}C_3H_7)_2\}_6]$ (d). The spinning frequency was 2 kHz (a, b, and d) or 3 kHz (c). Number of signal transients was 4 (b and d), 8 (c), and 16 (a). Centrebands are marked by *.

via the gauge-including atomic orbital (GIAO) method[21a,b] at the B3LYP level of theory. To examine the basis set dependence, an additional set of computations was performed using a 6-311+G(2d) basis set on phosphorus and all the atoms directly bound to it. The calculations were performed on an Origin 2000 Workstation equipped with four processors (Silicon Graphics, Inc.). Optimizations ranged from 1 to 5 days, while shielding computations were completed within 1−3 days. We anticipate that, for the full convergence of ^{31}P shielding tensor parameters, the P, S, and O atoms would probably require a quadruple-ζ basis with f-functions as has been shown necessary in calculations on the PH_3 system.[22] Calculations with such a basis are obviously outside the limit of our current computer resources.

3. Results and Discussion

3.1. ^{31}P CP/MAS NMR. Figure 3 shows ^{31}P CP/MAS NMR spectra of dialkyldithiophosphate compounds of potassium, nickel(II), and zinc(II) (see also Figures 1S−4S in Supporting Information). Spectra were obtained at two different spinning frequencies in order to distinguish the center bands, the positions of which give the isotropic chemical shifts for the phosphorus sites, as well as to perform an estimation of the ^{31}P CSA parameters from intensities of spinning sidebands with a higher confidence. Static ^{31}P NMR spectra were also recorded for a few samples to verify that the principal values of the ^{31}P CST estimated from the spinning sideband patterns are consistent with singularities observed in the powder patterns (see Figure 5S in Supporting Information). However, for static spectra with more than one magnetically nonequivalent phosphorus site, the certainty with which the CST principal values can be estimated from these singularities decreases dramatically because of an overlap of broad powder patterns. For these cases, only spinning sideband analysis can be used to estimate CSA parameters with a high confidence.

The potassium dialkyldithiophosphate salts are characterized by one or two nonequivalent phosphorus sites with isotropic shifts ranging from 103.8 to 115.4 ppm for various dialkyldithiophosphate ligands (see Table 2). The shape of the spinning sideband patterns is, however, very similar (see Figure 1S) because of similar CSAs (see Table 2). The nickel(II) dialkyldithiophosphate complexes have only one resonance line in ^{31}P CP/MAS NMR spectra at $\delta_{iso} = 90.7-94.9$ ppm (see Table 3, Figures 3b and 2S), flanked by spinning sidebands. The only exceptions are $[Ni\{S_2P(OC_3H_7)_2\}_2]$, which has two ^{31}P resonance lines due to the presence of two molecules in the unit cell,[2b] and $[\alpha\text{-}Ni\{S_2P(O\text{-}i\text{-}C_4H_9)_2\}_2]$, which has two ^{31}P resonance lines due to the presence of two nonequivalent ligands in the molecule.[2b] Knowing from the single-crystal X-ray diffraction studies that nickel(II) dialkyldithiophosphate complexes are mononuclear, the single resonance line in most of these compounds suggests a high symmetry and the chemical equivalence of the two terminal ligands in the complexes. CSAs of ^{31}P sites in these compounds are considerably smaller than those for the initial potassium salts, since the number of visible spinning sidebands and their intensities are smaller for spectra obtained at the same spinning frequencies. Also, the shape of the whole spectrum is mirror-imaged, which suggests a different sign of the CSA parameter δ_{aniso} and the skew of the CST, κ.

The binuclear zinc dialkyldithiophosphate complexes have two groups of resonances, with isotropic chemical shifts around 97−104 ppm and 93−100 ppm (see Table 4 and Figure 3S) that have been previously assigned to phosphorus sites in the bridging and the terminal ligands, respectively.[2f] The shape of the spinning sideband patterns for P-sites in the terminal ligands of the binuclear zinc(II) dialkyldithiophosphate complexes is very similar to the shape of the patterns in the MAS NMR spectra of the nickel(II) dialkyldithiophosphate complexes discussed above. The other spinning sideband patterns for P-sites in the bridging ligands of the binuclear zinc(II) dialkyldithiophosphate compounds are different and appear as almost a mirror image of the first ones. This empirical observation suggests that the CSAs of ^{31}P sites in the terminal and bridging ligands are very different. Moreover, if the shape of the CSA tensor is preserved from nickel to zinc complexes, this will confirm our previous assignment that the most shielded phosphorus sites in the zinc dialkyldithiophosphate complexes are the sites in the terminal ligands.

Figures 3d and 4S show ^{31}P CP/MAS NMR spectra of some tetranuclear zinc dialkyldithiophosphate complexes. In a few of these systems, the phosphorus sites in the six dialkyldithiophosphate ligands are nonequivalent (with isotropic shifts at 98.9−103.7 ppm) (see Table 5), but the shape of the spinning sideband patterns is generally the same for all sites. This shape is rather similar to that of the sideband pattern for the bridging ligands in the binuclear zinc(II) dialkyldithiophosphate complexes, which additionally supports our previous assignment.[2f]

3.2. ^{31}P Chemical Shift Anisotropy. Simulations of the ^{31}P CSA parameters were performed in the Mathematica program developed by Levitt and co-workers.[5] The results of these simulations for selected dialkyldithiophosphate compounds are displayed in Figure 4 as plots of joint confidence limits for δ_{aniso} and η. These ^{31}P CSA parameters, calculated as a mean of the

(21) (a) Ditchfield, R. *Mol. Phys.* **1974**, *27*, 789. (b) Wolinski, K.; Hinton, J. F.; Pulay, P. *J. Am. Chem. Soc.* **1990**, *112*, 8251.
(22) Wolinski, K.; Hsu, Ch.-L.; Hinton, J. F.; Pulay, P. *J. Chem. Phys.* **1993**, *99*, 7819.

Table 2. ^{31}P Chemical Shift Data for Potassium *O,O′*-Dialkyldithiophosphate Salts (95.4% Joint Confidence Limit for δ_{aniso} and η)

salt	δ_{iso} (ppm)	δ_{aniso} (ppm)[a]	η[a]	δ_{11} (ppm)	δ_{22} (ppm)	δ_{33} (ppm)	ν_r (kHz)
$KS_2P(OC_2H_5)_2$	108.5 ± 0.1	−107.6 ± 1.0	0.10 ± 0.06	168 ± 3	157 ± 7	0.9 ± 1.0	2+3
$KS_2P(OC_3H_7)_2$	114.7 ± 0.1	−106 ± 3	0.1 ± 0.1	172 ± 7	163 ± 16	9 ± 3	2+4
	114.5 ± 0.1	−109 ± 4	0.23 ± 0.14	181 ± 8	157 ± 18	6 ± 4	
$KS_2P(O\text{-}i\text{-}C_3H_7)_2$	111.7 ± 0.1	−104.7 ± 1.3	0.32 ± 0.03	180.6 ± 1.8	148 ± 4	7.0 ± 1.3	2+4
	103.8 ± 0.1	−116.7 ± 1.1	0.1 ± 0.1	166 ± 4	158 ± 9	−12.9 ± 1.1	
$KS_2P(OC_4H_9)_2$	115.4 ± 0.2	−106 ± 4	0.2 ± 0.2	177 ± 8	160 ± 18	9 ± 4	2+4
$KS_2P(O\text{-}i\text{-}C_4H_9)_2$	110.9 ± 0.2	−123.0 ± 2.0	0.0 ± 0.1	173 ± 9	172 ± 19	−12 ± 2	2+4
$KS_2P(O\text{-}s\text{-}C_4H_9)_2$	114.8 ± 0.6	−112.4 ± 1.7	0.33 ± 0.04	190 ± 3	153 ± 6	2.4 ± 1.9	3+4
	113.8 ± 0.4	−114.0 ± 1.0	0.28 ± 0.03	186.8 ± 1.7	155 ± 4	−0.2 ± 1.1	
$KS_2P(O\text{-}i\text{-}C_5H_{11})_2$	108.8 ± 0.5	−120 ± 2	0.1 ± 0.1	174 ± 6	164 ± 13	−11 ± 2	2+4
$KS_2P(O\text{-}c\text{-}C_6H_{11})_2$	109.3 ± 0.1	−110.6 ± 1.5	0.14 ± 0.10	172 ± 6	157 ± 12	−1.4 ± 1.5	2+4
	105.0 ± 0.1	−109.1 ± 1.7	0.21 ± 0.06	171 ± 3	148 ± 7	−4.1 ± 1.7	
mean[b]	111 ± 4	−112 ± 6	0.17 ± 0.11	176 ± 8	157 ± 14	−1 ± 7	

[a] See ref 13 for definitions of δ_{aniso} and η. [b] Statistical mean of parameters for these systems.

Table 3. ^{31}P Chemical Shift Data for Mononuclear Nickel(II) *O,O′*-Dialkyldithiophosphate Complexes (95.4% Joint Confidence Limit for δ_{aniso} and η)

complex	δ_{iso} (ppm)	δ_{aniso} (ppm)[a]	η[a]	δ_{11} (ppm)	δ_{22} (ppm)	δ_{33} (ppm)	ν_r (kHz)
$[Ni\{S_2P(OC_2H_5)_2\}_2]$	93.1 ± 0.1	58.4 ± 0.4	0.35 ± 0.04	151.5 ± 0.4	74 ± 3	53.7 ± 1.3	3+6
$[Ni\{S_2P(OC_3H_7)_2\}_2]$	94.8 ± 0.1	55.3 ± 0.8	0.40 ± 0.03	150.2 ± 0.8	78.2 ± 1.8	56.1 ± 0.9	1+3
	93.7 ± 0.1	53.5 ± 0.8	0.41 ± 0.03	147.1 ± 0.8	77.9 ± 1.8	55.9 ± 0.9	
$[Ni\{S_2P(O\text{-}i\text{-}C_3H_7)_2\}_2]$	93.3 ± 0.1	60.8 ± 0.9	0.48 ± 0.05	154.1 ± 0.9	77 ± 3	48.5 ± 1.5	2+4
$[Ni\{S_2P(OC_4H_9)_2\}_2]$[b]	93.0 ± 0.1						
α-$[Ni\{S_2P(O\text{-}i\text{-}C_4H_9)_2\}_2]$[c]	97.9 ± 0.1	59.4 ± 0.6	0.17 ± 0.06	157.2 ± 0.5	73 ± 4	63.0 ± 1.9	2+3
	96.0 ± 0.1	57.7 ± 0.5	0.05 ± 0.03	153.7 ± 0.5	69±2	65.9 ± 0.9	
β-$[Ni\{S_2P(O\text{-}i\text{-}C_4H_9)_2\}_2]$[d]	93.9 ± 0.1	54.6 ± 0.6	0.43 ± 0.06	148.6 ± 0.6	78 ± 4	54.9 ± 1.6	3+6
$[Ni\{S_2P(O\text{-}s\text{-}C_4H_9)_2\}_2]$	92.6 ± 0.6	63.6 ± 1.4	0.40 ± 0.10	156.2 ± 1.6	74 ± 8	48 ± 4	3+6
$[Ni\{S_2P(O\text{-}i\text{-}C_5H_{11})_2\}_2]$	94.9 ± 0.2	54.5 ± 0.8	0.31 ± 0.07	149.4 ± 0.8	76. ± 4	59 ± 2	2+3
$[Ni\{S_2P(O\text{-}c\text{-}C_6H_{11})_2\}_2]$	90.7 ± 0.2	55.9 ± 1.4	0.54 ± 0.12	146.6 ± 1.4	78 ± 8	48 ± 4	3+6
mean[e]	94 ± 2	57 ± 3	0.35 ± 0.15	152 ± 4	76 ± 10	55 ± 5	

[a] See ref 13 for definitions of δ_{aniso} and η. [b] Liquid. [c] Stable at $T < 296$ K, ref 2b. [d] Irreversible phase transition $\alpha \rightarrow \beta$ at $T > 313$ K, ref 2b. [e] Statistical mean of parameters for these systems.

values obtained at two different spinning frequencies, and the CST principal values, δ_{11}, δ_{22}, and δ_{33}, recalculated from δ_{aniso} and η, are presented in Tables 2−5 for all dialkyldithiophosphate systems studied. Figure 5a shows a correlation chart of the ^{31}P CSA parameters δ_{aniso} and η for the phosphorus sites in these systems. The chart shows that the data for different alkyl groups in the dialkyldithiophosphate ligands cluster together, depending on the type of the ligand in the compounds, i.e., the ionic, the terminal, or the bridging one, and depending on the type of the complex (mono-, bi-, or polynuclear). For example, the ^{31}P CSA parameters δ_{aniso} and η for all the nickel(II) dithiophosphate compounds containing only ligands of the terminal type form an "island" with $\delta_{aniso} \approx 54-64$ ppm and $\eta \approx 0.05-0.54$ (see Figure 5a).

^{31}P sites in the binuclear zinc(II) dialkyldithiophosphate complexes, which have been previously assigned to the terminal ligands,[2f] also have positive values of δ_{aniso} ($\delta_{aniso} \approx 48-61$ ppm) and η between 0 and 0.5 that cluster together with the data for the nickel(II) dialkyldithiophosphate compounds (see Figure 5a). In contrast, the ^{31}P sites of the bridging ligands in the both binuclear and tetranuclear zinc(II) dialkyldithiophosphate complexes have negative values of δ_{aniso} ($\delta_{aniso} \approx -47$ to -60 ppm), and the data cluster around two "islands" with $\eta \approx 0.1-0.5$ (for binuclear) and $\eta \approx 0.65-0.82$ (for tetranuclear complexes).

However, the most deshielded of the zinc(II) diethyldithiophosphate resonances differs from the bridging sites of the other ligands ($\delta_{aniso} = 46.0$ ppm, $\eta = 0.76$, see Table 4 and Figure 5a). As mentioned earlier, the zinc diethyldithiophosphate molecules form a polymeric chain with alternating terminal and bridging ligands. The phosphorus atom in the bridging ligands is in a different chemical environment than the phosphorus atoms in the bridging ligands of the binuclear compounds since the O_2PS_2 fragment has different geometries in the polynuclear and binuclear zinc(II) dialkyldithiophosphate complexes. Note, however, that for η close to 1, the sign of δ_{aniso} is uncertain. These changes in η are mostly determined by the principal value δ_{22} of the chemical shift tensor, which is usually the most sensitive to bond angles/lengths and to hydrogen-bonding and other intermolecular effects, as will be discussed later in this paper.

As was mentioned above, the tetranuclear zinc(II) dialkyldithiophosphate complexes have six ligands, all of the bridging type. For the ^{31}P sites in these ligands, δ_{aniso} has the same sign and the same order (-55 to -64 ppm) as that for the ^{31}P sites in the bridging ligands of the binuclear zinc(II) dialkyldithiophosphate complexes. However, η is somewhat larger ($\sim$0.65−0.82), which points to a higher rhombicity of ^{31}P CSTs in the tetranuclear Zn(II) dialkyldithiophosphate complexes compared with the binuclear ones. For the hexakis[μ_2-(*O,O′*-di-isopropyldithiophosphato-*S,S′*)]-μ_4-oxo-tetrazinc compound, all six ^{31}P sites are nonequivalent and well resolved in the ^{31}P NMR spectrum, with two groups of three resonance lines in each.[2f] However, simulations of the CSA parameters were performed for three peaks integrated together in each group (for the centerbands and corresponding sidebands) because of a poor resolution of the spinning sidebands farthest away from the centerbands, due to slight instabilities in the spinning frequency (±2 Hz). Therefore, CSA data are given for the two groups of ^{31}P resonance lines, and not for each of the six ^{31}P sites (see

Table 4. ^{31}P Chemical Shift Data for Polymeric and Binuclear Zinc(II) *O,O'*-Dialkyldithiophosphate Complexes (95.4% Joint Confidence Limit for δ_{aniso} and η)

complex	δ_{iso} (ppm)	δ_{aniso} (ppm)[a]	η[a]	δ_{11} (ppm)	δ_{22} (ppm)	δ_{33} (ppm)	ν_r (kHz)
$[Zn\{S_2P(OC_2H_5)_2\}_2]_\infty$	99.7 ± 0.2	46.0 ± 0.8	0.76 ± 0.09	145.7 ± 0.8	94 ± 5	59 ± 2	3+6
	95.6 ± 0.1	58.9 ± 0.5	0.29 ± 0.07	154.5 ± 0.6	75 ± 5	58 ± 2	
$[Zn_2\{S_2P(OC_3H_7)_2\}_4]$[b]	100.5 ± 0.1						
$[Zn_2\{S_2P(O\text{-}i\text{-}C_3H_7)_2\}_4]$	97.2 ± 0.1	−54.2 ± 1.4	0.2 ± 0.3	129 ± 9	120 ± 21	43.0 ± 1.4	3+6
	97.0 ± 0.1	−47 ± 3	0.4 ± 0.4	130 ± 10	111 ± 21	50 ± 3	
	93.0 ± 0.1	51.6 ± 0.8	0.2 ± 0.2	144.6 ± 0.8	72 ± 13	63 ± 6	
$[Zn_2\{S_2P(OC_4H_9)_2\}_4]$[b]	100.5 ± 0.1						
$[Zn_2\{S_2P(O\text{-}i\text{-}C_4H_9)_2\}_4]$	103.7 ± 0.1	−57.0 ± 1.8	0.34 ± 0.12	142 ± 4	122 ± 8	46.6 ± 1.8	1.5+3
	103.1 ± 0.1	−54.6 ± 1.9	0.41 ± 0.12	142 ± 4	119 ± 7	48.5 ± 1.9	
	100.1 ± 0.1	57.1 ± 1.6	0.1 ± 0.2	157.2 ± 1.6	75 ± 12	69 ± 5	
	99.5 ± 0.1	57.0 ± 1.5	0.1 ± 0.2	156.5 ± 1.6	73 ± 10	69 ± 5	
$[Zn_2\{S_2P(O\text{-}s\text{-}C_4H_9)_2\}_4]$	98.0 ± 0.3	−48.5 ± 0.7	0.42 ± 0.04	132.3 ± 1.2	112 ± 3	49.5 ± 0.8	2+3
	97.5 ± 0.2	−48.6 ± 1.0	0.29 ± 0.11	129 ± 3	115 ± 6	49 ± 1	
	95.9 ± 0.3	50 ± 4	0.1 ± 0.3	146 ± 4	72 ± 16	70 ± 7	
	95.4 ± 0.3	48.2 ± 1.7	0.2 ± 0.2	143.6 ± 1.7	75 ± 13	67 ± 6	
$[Zn_2\{S_2P(O\text{-}i\text{-}C_5H_{11})_2\}_4]$	103.9 ± 0.1	−57.4 ± 0.7	0.30 ± 0.05	141.1 ± 1.6	124 ± 3	46.5 ± 0.7	2+3
	103.4 ± 0.1	−59.6 ± 0.5	0.47 ± 0.02	147.1 ± 0.6	119.3 ± 1.1	43.8 ± 0.5	
	97.7 ± 0.1	50.8 ± 0.7	0.14 ± 0.12	148.5 ± 0.7	76 ± 7	69 ± 3	
	97.4 ± 0.1	49.9 ± 0.5	0.20 ± 0.10	147.3 ± 0.5	77 ± 5	68 ± 2	
	97.2 ± 0.1	52.7 ± 1.0	0.1 ± 0.2	149.9 ± 1.1	75 ± 11	67 ± 5	
	97.1 ± 0.1	51.9 ± 0.9	0.1 ± 0.2	149.0 ± 0.9	74 ± 11	69 ± 5	
$[Zn_2\{S_2P(O\text{-}c\text{-}C_6H_{11})_2\}_4]$	99.7 ± 0.2	−47.9 ± 1.2	0.41 ± 0.08	134 ± 2	114 ± 4	51.8 ± 1.2	2
$T < 316$ K[c]	99.5 ± 0.1	−49.4 ± 1.4	0.50 ± 0.07	137 ± 2	112 ± 4	50.1 ± 1.4	
	97.3 ± 0.2	61.4 ± 0.6	0.23 ± 0.04	158.7 ± 0.6	74 ± 3	59.5 ± 1.3	
$[Zn_2\{S_2P(O\text{-}c\text{-}C_6H_{11})_2\}_4]$	99.3 ± 0.1	−54.3 ± 1.6	0.1 ± 0.3	129 ± 9	124 ± 20	45.0 ± 1.6	3+6
$T > 316$ K[c]	98.0 ± 0.1	−52 ± 3	0.4 ± 0.3	133 ± 9	115 ± 19	46 ± 3	
	95.3 ± 0.1	52 ± 2	0.4 ± 0.3	147 ± 2	81 ± 17	58 ± 8	
	93.9 ± 0.1	50 ± 2	0.5 ± 0.3	144 ± 2	80 ± 17	58 ± 8	
mean terminal[d]	96.6 ± 2.0	53.1 ± 4.1	0.19 ± 0.14	149.6 ± 4.5	75.0 ± 8.9	65 ± 5	
mean bridging[e]	100.5 ± 2.8	−53.4 ± 4.5	0.35 ± 0.12	136.5 ± 5.3	118.0 ± 8.6	47 ± 5	

[a] See ref 13 for definitions of δ_{aniso} and η. [b] Liquid. [c] Phase transition from a low-temperature conformation with C_i symmetry to a high-temperature distorted conformation. [d] Statistical mean of parameters for the terminal ligands. [e] Statistical mean of parameters for the bridging ligands (data for $[Zn\{S_2P(OC_2H_5)_2\}_2]_\infty$ were omitted because of its polynuclear structure).

Table 5. ^{31}P Chemical Shift Data for Tetranuclear Hexakis[μ_2-(*O,O'*-dialkyldithiophosphato-*S,S'*)]-μ_4-oxo-tetrazinc Complexes (95.4% Joint Confidence Limit for δ_{aniso} and η)

complex	δ_{iso} (ppm)	δ_{aniso} (ppm)[a]	η[a]	δ_{11} (ppm)	δ_{22} (ppm)	δ_{33} (ppm)	ν_r (kHz)
$[Zn_4O\{S_2P(OC_2H_5)_2\}_6]$	102.2 ± 0.6	−58 ± 5	0.82 ± 0.11	155 ± 5	108 ± 9	44 ± 5	2+3
	100.9 ± 0.6	−58 ± 2	0.79 ± 0.07	152 ± 3	107 ± 5	43 ± 2	
	100.0 ± 0.5	−64 ± 6	0.76 ± 0.15	156 ± 7	108 ± 12	36 ± 6	
$[Zn_4O\{S_2P(OC_3H_7)_2\}_6]$	102.7 ± 0.4	−59.1 ± 1.5	0.74 ± 0.15	154 ± 5	110 ± 10	43.7 ± 1.5	2+3
$[Zn_4O\{S_2P(O\text{-}i\text{-}C_3H_7)_2\}_6]$[b]	100.2 ± 0.5	−61 ± 3	0.70 ± 0.10	152 ± 4	110 ± 8	40 ± 3	2+3
	98.9 ± 0.5	−56 ± 3	0.81 ± 0.12	149 ± 5	104 ± 9	43 ± 3	
$[Zn_4O\{S_2P(OC_4H_9)_2\}_6]$	103.7 ± 0.2	−60 ± 3	0.68 ± 0.12	154 ± 4	113 ± 9	44 ± 3	3+4.5
	103.2 ± 0.2	−61 ± 3	0.65 ± 0.11	154 ± 4	114 ± 8	42 ± 3	
mean[c]	101.5 ± 1.7	−60 ± 3	0.74 ± 0.06	153 ± 5	109 ± 5	42 ± 3	

[a] See ref 13 for definitions of δ_{aniso} and η. [b] The spectrum contains two groups of resonances with three resonances in each group, 98.7, 99.0, 99.1 and 100.0, 100.3, 100.5. In this study the CSA values δ_{aniso} and η were simulated by integrating over each group. [c] Statistical mean of parameters for these complexes.

Table 5). However, the intensities of the spinning sidebands and, therefore, the CSA parameters for these ^{31}P sites are very close to each other, and our approach seems to be reliable.

Figure 5b shows a stick diagram of the mean ^{31}P CST principal values δ_{11}, δ_{22}, and δ_{33} for the different types of dialkyldithiophosphate compounds revealing the general shape of the ^{31}P CSTs. The mean is calculated from data for ^{31}P sites in different alkyl groups in the dialkyldithiophosphate ligands. ^{31}P sites of the ionic salts have the largest span, $\Omega \approx 180$ ppm. The CSTs are almost axially symmetric ($\delta_{11} \approx \delta_{22}$), with the skew, κ, close to +1. The terminal ligands of both nickel(II) and zinc(II) dialkyldithiophosphates have almost the same type of ^{31}P CSTs, with κ close to −1. The ^{31}P CSTs for the bridging ligands of the binuclear zinc(II) dialkyldithiophosphate compounds are similar to the ^{31}P CSTs for the tetranuclear compounds, though the rhombicity of these tensors for the latter compounds is larger ($\eta_{mean} = 0.35$ and 0.74 for the bridging ligands in zinc(II) binuclear and zinc(II) tetranuclear dialkyldithiophosphate complexes, respectively). The tensors for the structurally different bridging and terminal ligands in the binuclear compounds are the mirror images of each other, predominantly due to large differences in δ_{22} (see Figure 5b). Therefore, it is interesting to investigate the relationship between the known structure for these different types of ligands in the dialkyldithiophosphate complexes and the principal value components of the ^{31}P chemical shift tensors. Both the analysis of the single-crystal structures obtained from the X-ray diffraction data and ab initio calculations of the full ^{31}P CST will be used for this purpose.

Figure 6 shows plots of the principal values of ^{31}P CSTs versus different structural parameters of the Zn(II) and Ni(II) dialkyldithiophosphate complexes with known single-crystal

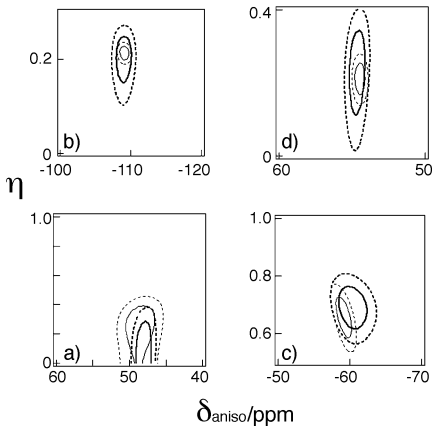

Figure 4. χ^2 statistics as a function of the CSA parameters δ_{aniso} and η. Graphs for representative ^{31}P sites in four *O,O′*-dialkyldithiophosphate systems are presented: (a) $[Zn_2\{S_2P(O\text{-}s\text{-}C_4H_9)_2\}_4]$ (δ_{iso} = 95.4 ppm, ν_r = 3 kHz (thin lines), and 1.5 kHz (thick lines)); (b) $KS_2P(O\text{-}c\text{-}C_6H_{11})_2$ (δ_{iso} = 105.0 ppm, ν_r = 2 kHz (thin lines), and 4 kHz (thick lines)); (c) $[Zn_4O\{S_2P(O{-}C_4H_9)_2\}_6]$ (δ_{iso} = 103.7 ppm, ν_r = 4.5 kHz (thick lines), and 3 kHz (thin lines)); and (d) $[Ni\{S_2P(O\text{-}i\text{-}C_5H_{11})_2\}_2]$ (δ_{iso} = 94.9 ppm, ν_r = 2 kHz (thin lines), and 3 kHz (thick lines)). The 68.3% joint confidence limit (solid lines) and 95.4% joint confidence limit (dashed lines) for the two CSA parameters are shown.

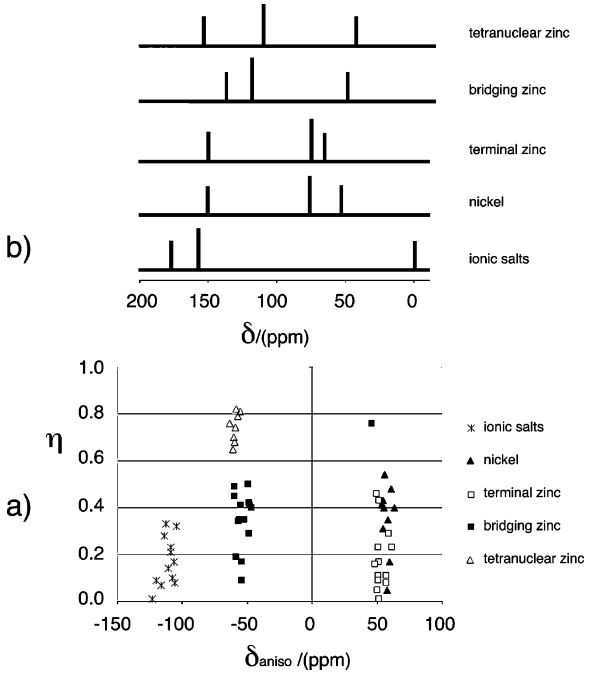

Figure 5. Correlation chart for the ^{31}P CSA parameters δ_{aniso} and η (a) and a stick diagram of the mean ^{31}P CST principal values, δ_{11}, δ_{22}, and δ_{33} (b) for the dialkyldithiophosphate compounds.

X-ray diffraction structures. Obviously, experimental values for the CST principal component δ_{22} increase with an increase of both S−P−S and O−P−O angles. The terminal ligands have smaller S−P−S angles (102−110°) than the bridging ligands (108−121°) (see Table 1), and the δ_{22} principal component of the ^{31}P CST changes more than 50 ppm, while δ_{11} and δ_{33} are almost unchanged (see Figure 6c). Eventually, δ_{aniso} and κ change the sign because $\delta_{22} > \delta_{iso}$ for the bridging ligands while $\delta_{22} < \delta_{iso}$ for the terminal ones (see also Figure 5b). Note that the S−P−S angles in both the bridging and the terminal ligands in the polymeric zinc(II) diethyldithiophosphate complex are very similar (see Table 1) and correlate with close values of δ_{22} for P-sites in these structurally different dialkyldithiophosphate ligands.

However, despite the visible correlations between the values for δ_{22} and S−P−S and O−P−O bond angles (see Figure 6c,d), it is difficult to conclude from experimental data which of the two angles has a predominant influence on δ_{22}, since both angles vary simultaneously in the S_2PO_2 molecular fragment of the dithiophosphate compounds. As will be shown by ab initio calculations, it is the S−P−S and *not* the O−P−O bond angle that has the dominating effect on variations of the δ_{22} component. There does not seem to be any significant correlation between either P−O or P−S bond lengths and the principal values of the ^{31}P CST. However, experimental observation of such correlations might be difficult since the ranges of the bond lengths in the dialkyldithiophosphate compounds under study are rather narrow (0.03 and 0.04 Å for P−O and P−S, respectively).

3.3. Ab Initio Calculations. $[(CH_3O)_2PS_2]^-$ Molecular Fragment. The ^{31}P isotropic shielding, its three principal shielding components, span, skew, δ_{aniso}, and η, obtained at various values of P−O and P−S bond lengths, and O−P−O and S−P−S bond angles for $[(CH_3O)_2PS_2]^-$ are presented in Tables 6−8.

Table 6 displays the bond length dependence. The calculated equilibrium values for these parameters are 1.66 Å (P−O bond) and 2.00 Å (P−S bond). The isotropic shielding values shift in response to the varying bond length. The derivatives at the equilibrium geometry are calculated to be −160 and −230 ppm/Å for the P−O and P−S bonds, respectively. Additional calculations in which the P−S and P−O bonds are varied simultaneously indicate that the bond length effects are additive (data not shown). The span of the tensor increases with these two bond lengths, owing to the dramatic dependence of the least shielded component, σ_{11}. On the other hand, differences in the bond length apparently cannot change the shape of the shielding tensor, because the sign of the anisotropy in all cases remains the same, while the changes in the intermediate component, σ_{22}, follow closely the changes in σ_{11}.

The effects of the O−P−O bond angle on the ^{31}P shielding tensor are presented in Table 7. The calculated results do not exhibit a monotonic dependence of the principal components on this bond angle. Instead, the isotropic shielding appears to have reached a maximum value in the vicinity of the O−P−O bond angle at 100°. The behavior of each principal component can also be quite different from that of the isotropic shielding. For example, σ_{11} seems to have a maximum around a O−P−O bond angle of 96°. In contrast, σ_{22} shows a minimum at this angle. Finally, σ_{33} seems to be the least affected component, changing monotonically, i.e., increasing with decreasing O−P−O angle. δ_{aniso} calculated from the shielding principal components, while remaining negative, changes only slightly, with the absolute value increasing slowly with decreasing O−P−O bond angle. The span of the tensor, as expected, does not have a monotonic dependence. The width of the tensor is suggested to have a minimum around a O−P−O bond angle of 100°.

Table 8 shows the dependence of the ^{31}P shielding tensor on the S−P−S bond angle. In contrast to the O−P−O bond angle dependence, the principal components σ_{22} and σ_{33} both change monotonically with the S−P−S bond angle. Furthermore, as this bond angle is reduced, σ_{33} decreases while σ_{22} does the

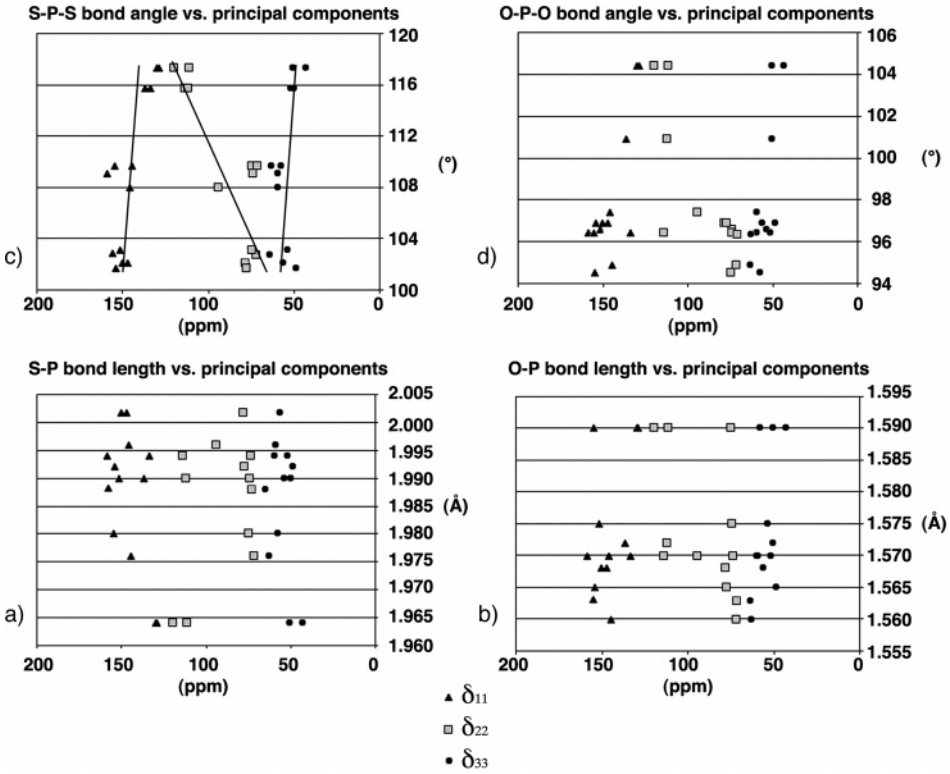

Figure 6. Chemical shift tensor principal values versus S−P (a) and O−P (b) bond lengths, and S−P−S (c) and O−P−O (d) bond angles obtained from known X-ray diffraction structures for Ni(II) and Zn(II) dialkyldithiophosphate complexes. Solid lines are guides to the eye.

Table 6. Calculated ^{31}P Chemical Shielding Tensors (ppm) as a Function of P−O and P−S Bond Lengths in $[(CH_3O)_2PS_2]^-$ Molecular Fragment

bond length[a] (Å)	σ_{iso}	σ_{11}	σ_{22}	σ_{33}	Ω	κ	δ_{aniso}	η
P−O								
1.61	220.3	129.0	164.0	368.0	239.0	0.707	−147.7	0.237
1.65	207.7	109.0	145.9	368.2	259.2	0.715	−160.5	0.230
1.66	204.5	104.1	141.3	368.2	264.1	0.718	−163.7	0.227
1.67	201.3	99.2	136.6	368.2	269.0	0.722	−166.9	0.224
1.71	188.5	79.9	117.6	367.9	288.0	0.738	−179.4	0.210
P−S								
1.95	226.0	127.7	165.5	384.8	257.1	0.706	−158.8	0.238
1.99	208.9	109.0	146.2	371.5	262.5	0.717	−162.6	0.229
2.00	204.5	104.1	141.3	368.2	264.1	0.718	−163.7	0.227
2.01	200.0	99.11	136.2	364.8	265.7	0.720	−164.8	0.225
2.05	181.8	78.71	115.5	351.3	272.6	0.730	−169.5	0.217

[a] Bond lengths in the B3LYP optimized structures.

Table 7. Calculated ^{31}P Chemical Shielding Tensors (ppm) as a Function of O−P−O Bond Angle in $[(CH_3O)_2PS_2]^-$ Molecular Fragment

O–P–O bond angle (deg)[a]	σ_{iso}	σ_{11}	σ_{22}	σ_{33}	Ω	κ	δ_{aniso}	η
108.6	202.7	82.4	171.1	354.7	272.3	0.348	−152.0	0.584
104.5	203.8	101.2	152.9	357.2	256.0	0.596	−153.4	0.337
100.3	204.1	116.9	135.3	360.0	243.1	0.849	−155.9	0.118
96.1	203.9	118.5	129.7	363.4	244.9	0.909	−159.5	0.070
91.8	203.4	102.7	139.8	367.8	265.1	0.720	−164.4	0.226
87.4	202.6	86.1	148.1	373.6	287.5	0.569	−171.0	0.363

[a] Bond angles in the B3LYP optimized structures

opposite. The intermediate component, σ_{22}, which defines the shape of the tensor, is seen to depend strongly on the S−P−S bond angle. This component lies normal to the plane defined by the metal center, phosphorus, and sulfur atoms. The isotropic value remains relatively constant as the bond angle changes, yet this does not hold true for the span and the principal components. As the bond angle decreases, the tensor span also decreases. The most interesting feature, not observed with the other geometric parameters, is an apparent change in the sign of both the skew and δ_{aniso}. For the specific model employed in these calculations, δ_{aniso} changes sign between S−P−S bond angles of 95° and 98°. The precise angle at which δ_{aniso} changes sign is expected to depend on several factors, including the identity of the metal center and the ligands. However, it can be stated from these calculations that larger S−P−S angles are expected to yield tensors with negative δ_{aniso} values, while smaller angles will tend toward positive values. Within the relevant range of 93−125°, as the bond angle increases, σ_{22} decreases while both σ_{11} and σ_{33} increase. The rate at which each component changes with the S−P−S angle depends on the component. The least shielded component, σ_{11}, shifts at a slower rate than the other two components. Figure 7 illustrates the change in the shape of the shielding tensor as the S−P−S

Table 8. Calculated ^{31}P Chemical Shielding Tensors (ppm) as a Function of S−P−S Bond Angle in $[(CH_3O)_2PS_2]^-$ Molecular Fragment

S–P–S bond angle (deg)	σ_{iso}	σ_{11}	σ_{22}	σ_{33}	Ω	κ	δ_{aniso}	η
125	202.8	102.0	126.4	380.0	278.0	0.824	−177.2	0.138
120	203.4	102.6	139.3	368.3	265.7	0.724	−164.9	0.223
115	203.6	102.9	151.7	356.1	253.2	0.615	−152.5	0.320
98	201.8	95.9	198.5	310.9	215.0	0.046	−109.1	0.940
95	201.2	91.9	209.5	302.3	210.4	−0.118	109.3	0.849
93	200.9	88.3	217.8	296.5	208.2	−0.244	112.6	0.699

[a] Bond angles in the B3LYP optimized structures.

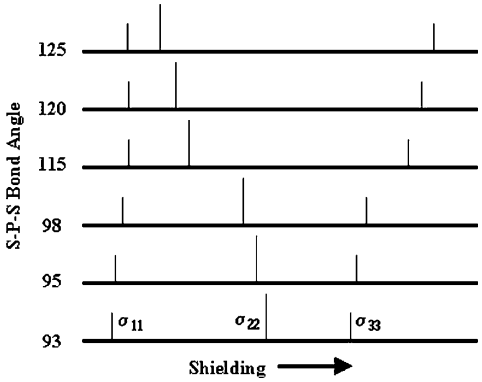

Figure 7. Stick diagram showing the dependence of the calculated principal components of the ^{31}P shielding tensor in the model fragment $[(CH_3O)_2PS_2]^-$ on the S−P−S bond angle.

angle is varied. As the bond angle increases, σ_{22} decreases and δ_{aniso} becomes negative; that is, σ_{22} is now closer to σ_{11} than it is to σ_{33}. With this observation in mind, a possible interpretation may be suggested to explain the experimental trends.

Ni(II) and Zn(II) Dialkyldithiophosphate Compounds. After geometry optimization, the S−P and P−O bond lengths in the calculated dialkyldithiophosphate compounds range from 1.98 to 2.05 Å and from 1.60 to 1.62 Å, respectively. These ranges are still relatively large and are predicted to cause large fluctuations in the calculated shielding values. The P−S and P−O bond lengths in the complexes obtained from the optimization calculations were slightly longer than those suggested by the X-ray data. The patterns for the other geometric parameters observed in the X-ray data are mirrored in the ab initio geometry optimization results. For example, a trend seen in both X-ray and theoretical structures is that the S−P−S bond angle in the tetranuclear hexakis[μ_2-(*O*,*O*′-diethyldithiophosphato-*S*,*S*′)]-μ_4-thio-tetrazinc molecule (121.1°) is larger than in all the other species described in this paper. The other compounds have S−P−S bond angles ranging from 104.4° to 117.4° for both terminal and bridging ligands. The tetranuclear compound differs from the remaining complexes in that the phosphorus atom does not participate in a rigid four-membered planar ring, and this allows the S−P−S angle to adopt larger values. Similarly, the O−P−O bond angles in each dialkyldithiophosphate complex are smaller than the S−P−S bond angles, a characteristic feature found in both theoretical and experimental results.

Without doubt, the environment of the phosphorus atom greatly influences its shielding tensor. The dialkyldithiophosphates in this paper contain either terminal or bridging ligands. Experimentally, it appears that the shape of the shielding tensor differs depending on this aspect of the ligand, whether it is terminal or bridging. Terminal ligands have positive δ_{aniso} while bridging ligands have negative δ_{aniso}. Tables 9 (terminal ligands) and 10 (bridging ligands) show the calculated isotropic shielding, its three principal components of the shielding tensor, Ω, κ, δ_{aniso}, and η for selected Zn(II) and Ni(II) dialkyldithiophosphate compounds using two basis sets, 6-31G** and 6-311+G(2d). They also include the S−P−S bond angle of the P atom of interest, taken from the optimized geometry.

The basis set comparison shows that these calculations are not yet saturated in the basis functions. However, if one compares the isotropic shielding values between the two basis sets, there seems to be a constant offset. Unfortunately, with regard to the tensor quantities such as skew and δ_{aniso}, this offset is not as nearly constant. Nonetheless, one qualitative trend is obvious with both basis sets. Terminal ligands have ^{31}P shielding tensors described by a negative skew (positive δ_{aniso}), while bridging ligands are characterized by tensors with a positive skew (negative δ_{aniso}). The Ω values of these tensors also vary depending on the nature of the ligand. Terminal ligands generally have smaller Ω than do the bridging ligands.

Tables 9 and 10 show that the terminal ligands have smaller S−P−S bond angles than the bridging ligands. This trend was also seen in the analysis of the model fragment in which small S−P−S bond angles lead to positive δ_{aniso} values. On the basis of the calculations, the component σ_{22} lies normal to the plane of the S−P−S angle; thus, an alteration in this bond angle will affect σ_{22} strongly and thereby change the shape of the tensor.

The agreement between theoretical and experimental values in Tables 9 and 10 is not perfect, although it is promising. Nevertheless, trends obtained from these calculations already agree with those based on experiment. The big discrepancy between calculations and experiment for the bridging ligand in the zinc(II) diethyldithiophosphate complex can be explained on the basis of the different structures. The calculations were performed on a model fragment with the same type of terminal and bridging ligands as the binuclear zinc(II) di-isopropyldithiophosphate complex, but in fact the zinc(II) diethyldithiophosphate compound forms a polymeric chain, in which the bridging ligands have a very different geometric environment compared with the binuclear case.

To test further possible reasons for the discrepancy between calculations and experiment, we also performed additional calculations: (i) On one selected dialkyldithiophosphate compound, $[Ni\{S_2P(OC_2H_5)_2\}_2]$, the DZ basis set was used on the Ni atom to test if the minimal basis that comes with LANL1MB ECP employed on the metal atoms is too small. As can be seen in Table 9 (bottom), the effects of this basis on the ^{31}P CST parameters are much smaller than the effects of the basis on P, S, and O atoms. The latter atoms probably require quadruple-ζ basis with f-functions,[22] which is outside the limits of our current computer resources. (ii) ^{31}P CST data given in Tables 9 and 10 were obtained by calculations for isolated molecules, neglecting effects of the surrounding crystal matrix. To test whether the long-range electrostatic interactions are a source of the errors of the computed data with respect to experiment, additional calculations for the $[S_2P(OCH_3)_2]^-$ molecular fragment were performed: +0.5 atomic unit charge was placed 3.5 Å away from the S atom along the axis containing the P−S bond that models the long-range electrostatic interaction in the crystal matrix. Calculations showed only minor changes on the ^{31}P chemical shielding parameters: $\Delta\sigma_{iso} = +3.85$ (∼2%), $\Delta\sigma_{11} = +10.88$ (∼10%), $\Delta\sigma_{22} = +5.16$ (∼2.5%), and $\Delta\sigma_{33} = -4.49$ ppm (∼ −1.5%). Arranging two +0.5 atomic unit charges symmetrically 3.5 Å away from the S atoms along the axes containing the two P−S bonds gave only negligible changes in the calculated chemical shielding parameters: ($\Delta\sigma_{iso}$, $\Delta\sigma_{11}$, $\Delta\sigma_{22}$, $\Delta\sigma_{33}$) = (+0.0006, −0.0041, 0.0076, −0.0017) ppm.

Orientation of the ^{31}P CST Principal Axis System with Respect to the O_2PS_2 Molecular Fragment. Results of ab initio calculations for Ni(II) and Zn(II) dialkyldithiophosphate complexes allowed us to examine the orientation of the ^{31}P CST principal axes system with respect to the O_2PS_2 molecular

Table 9. Calculated ^{31}P Chemical Shielding Tensors (ppm) for Terminal Ligands in *O,O′*-Dialkyldithiophosphate Ni(II) and Zn(II) Complexes, with Data in Parentheses Obtained from Experimental Results

	S–P–S bond angle (deg)[a]	σ_{iso}	σ_{11}	σ_{22}	σ_{33}	Ω	κ	δ_{aniso}	η
				6-31G** Basis on P, S, and O					
$[Zn_2\{S_2P(O\text{-}i\text{-}C_3H_7)_2\}_4]$	109.5	225.4	168.9	249.9	257.3	88.4	−0.831	56.5	0.131
						(81.8)	(−0.785)	(51.6)	(0.17)
$[Zn\{S_2P(OC_2H_5)_2\}_2]_\infty$	110.35	227.3	178.2	249.0	254.8	76.6	−0.850	49.1	0.118
						(96.9)	(−0.650)	(58.9)	(0.29)
$[Ni\{S_2P(O\text{-}i\text{-}C_3H_7)_2\}_2]$	104.43	229.9	172.8	256.4	260.6	87.8	−0.905	57.1	0.074
						(105.6)	(−0.452)	(60.8)	(0.48)
$[Ni\{S_2P(OC_2H_5)_2\}_2]$	105.16	233.0	181.6	247.5	269.8	88.2	−0.493	51.4	0.433
						(97.8)	(−0.580)	(58.4)	(0.35)
				6-311+G(2d) Basis on P, S, and O					
$[Zn_2\{S_2P(O\text{-}i\text{-}C_3H_7)_2\}_4]$	109.5	153.3	82.4	187.7	189.8	107.4	−0.961	70.9	0.030
						(81.8)	(−0.785)	(51.6)	(0.17)
$[Zn\{S_2P(OC_2H_5)_2\}_2]_\infty$	110.3	156.6	95.7	181.6	192.4	96.7	−0.776	60.9	0.177
						(96.9)	(−0.650)	(58.9)	(0.29)
$[Ni\{S_2P(O\text{-}i\text{-}C_3H_7)_2\}_2]$	104.5	159.2	87.5	192.0	198.0	110.5	−0.890	71.7	0.084
						(105.6)	(−0.452)	(60.8)	(0.48)
$[Ni\{S_2P(OC_2H_5)_2\}_2]$	105.1	161.5	100.6	176.2	207.8	107.2	−0.411	60.9	0.519
						(97.8)	(−0.580)	(58.4)	(0.35)
				6-311+G(2d) Basis on P, S, and O and DZ Basis on Ni					
$[Ni\{S_2P(OC_2H_5)_2\}_2]$	105.1	172.2	102.2	181.1	233.3	131.1	−0.204	70.0	0.745
						(97.8)	(−0.580)	(58.4)	(0.35)

[a] Mean of bond angles in the B3LYP optimized structures.

Table 10. Calculated ^{31}P Chemical Shielding Tensors (ppm) for Bridging Ligands in *O,O′*-Dialkyldithiophosphate Zn(II) Complexes, with Data in Parentheses Obtained from Experimental Results

	S–P–S bond angle (deg)[a]	σ_{iso}	σ_{11}	σ_{22}	σ_{33}	Ω	κ	δ_{aniso}	η
				6-31G** Basis on P, S, and O					
$[Zn_2\{S_2P(O\text{-}i\text{-}C_3H_7)_2\}_4]$	113.9	235.4	183.6	234.1	288.4	104.8	0.035	−53.0	0.954
						(85.9)	(0.786)	(−54.2)	(0.17)
		238.4	200.9	225.8	288.6	87.7	0.432	−50.2	0.496
						(79.5)	(0.536)	(−46.8)	(0.40)
$[Zn_4S\{S_2P(OC_2H_5)_2\}_6]$	121.4	235.0	173.5	218.3	313.0	139.5	0.359	−78.1	0.574
$[Zn\{S_2P(OC_2H_5)_2\}_2]_\infty$	117.4	220.0	146.0	158.7	355.2	209.2	0.879	−135.2	0.094
						(86.6)	(−0.190)	(46.0)	(0.76)
				6-311+G(2d) Basis on P, S, and O					
$[Zn_2\{S_2P(O\text{-}i\text{-}C_3H_7)_2\}_4]$	113.9	152.4	96.8	144.0	216.3	119.5	0.211	−64.0	0.737
						(85.9)	(0.786)	(−54.2)	(0.17)
		157.1	116.1	139.7	215.6	99.5	0.526	−58.5	0.403
						(79.5)	(0.536)	(−46.8)	(0.40)
$[Zn_4S\{S_2P(OC_2H_5)_2\}_6]$	121.4	154.1	89.1	130.9	242.2	153.1	0.455	−88.1	0.474
$[Zn\{S_2P(OC_2H_5)_2\}_2]_\infty$	117.4	137.5	60.7	72.3	279.4	218.7	0.894	−141.9	0.082
						(86.6)	(−0.190)	(46.0)	(0.76)

[a] Mean of bond angles in the B3LYP optimized structures.

fragment. Note that such information is needed for structural studies on amorphous and powder systems using novel solid-state NMR techniques, for example, torsion angle measurements.[23]

In the undistorted geometry of the model $[(CH_3O)_2PS_2]^-$ fragment, the principal axis bound with the σ_{33} element of the ^{31}P CST bisects the S−P−S bond angle, the principal axis of the σ_{11} element is perpendicular to that of σ_{33} and lies in the same plane, and the principal axis bound with σ_{22} is orthogonal to both of these other principal axes. To determine how large the deviations of the ^{31}P CST principal axes frame from this geometry are in the optimized structures of the Zn(II) and Ni(II) dialkyldithiophosphate complexes, the three directional vector components of the CST given in the calculations were compared with the directional vector components of the tensor that would have been, were the geometry not distorted (i.e., as in the model $[(CH_3O)_2PS_2]^-$ fragment). The deviations in the geometry were assumed to be so small that the same atomic coordinates as in the optimized geometry could be used. The calculated deviations are presented in Table 11. In each case, the P sites in both Ni(II) and Zn(II) dialkyldithiophosphate complexes are nonequivalent, which gives more than one tensor orientation for each complex. In some cases the tensor is almost axially symmetric; therefore, the directions of the two tensor components that have close values are no longer reliable. In an undistorted O_2PS_2 tetrahedron, the S−S vector (**S**) is perpendicular to the O−O vector (**O**). Deviations from this tetrahedral geometry due to metal bonding were also calculated as $\phi = \arccos\{(\mathbf{O},\mathbf{S})/|\mathbf{O}|\,|\mathbf{S}|\}$.

(23) Antzutkin, O. N. In *Solid State NMR Spectroscopy Principles and Applications*; Duer, M. J., Ed.; Blackwell Science Ltd.: Oxford, 2002; p 280.

Table 11. Deviations between Geometries of the Undistorted ^{31}P Chemical Shift Tensor (in the Model $[(CH_3O)_2PS_2]^-$ Fragment) and the Tensor Distorted Due to Bonding to Metal Atoms in Calculated Ni(II) and Zn(II) Dithiophosphate Complexes

	terminal ligands				bridging ligands			
complex	Δ_{11} (deg)[1]	Δ_{22} (deg)[1]	Δ_{33} (deg)[a]	ϕ (deg)[b]	Δ_{11} (deg)[a]	Δ_{22} (deg)[a]	Δ_{33} (°)[a]	ϕ (deg)[b]
$[Ni\{S_2P(OC_2H_5)_2\}_2]$	1.3	1.3	0	0				
6-31G**	0	0.6	0	0				
$[Ni\{S_2P(O\text{-}i\text{-}C_3H_7)_2\}_2]$	10.4[c]	10.4[c]	0.5	0.2				
6-311+G(2d)	10.5[c]	10.5[c]	0	0.2				
$[Zn_2\{S_2P(O\text{-}i\text{-}C_3H_7)_2\}_2]$	14.8[c]	14.1[c]	5.2	0.2	7.3	13.9	14.4	3.4
6-31G**	4.4[c]	3.4[c]	4.0	0.4	15.0	17.2	21.3	3.3
$[Zn_2\{S_2P(O\text{-}i\text{-}C_3H_7)_2\}_2]$	41.8[c]	41.6[c]	4.6	0.2	6.0	17.5	17.6	3.4
6-311+G(2d)	24.8[c]	24.6[c]	3.7	0.4	11.8	22.1	23.6	3.3
$[Zn_4S\{S_2P(OC_2H_5)_2\}_6]$					10.7	20.5	19.0	4.6
6-31G**					11.2	19.0	17.3	4.6
					9.8	19.5	18.4	4.2
					9.5	23.0	22.6	4.0
					8.7	22.6	22.3	3.9
					11.5	19.2	16.4	4.8

[a] $\Delta_{nn} = \arccos\{(\sigma_{nn}^{dist},\sigma_{nn}^{undist})/|\sigma_{nn}^{dist}|\,|\sigma_{nn}^{undist}|\}$. [b] $\phi = \arccos\{(\mathbf{O},\mathbf{S})/|\mathbf{O}|\,|\mathbf{S}|\}$. [c] Can be disregarded due to almost axially symmetric ^{31}P CSTs.

In ab initio calculations for the zinc(II) and nickel(II) dialkyldithiophosphate complexes, deviations from the geometry of the principal axis frame of the ^{31}P CST of the model molecule $[(CH_3O)_2PS_2]^-$ were less than 5.2° for the terminal ligands in the mononuclear nickel(II) and binuclear zinc(II) complexes. For the bridging ligands in the binuclear and tetranuclear zinc-(II) complexes, the deviations were between 6° and 23.6°.

4. Conclusions

^{31}P NMR data, i.e., isotropic chemical shifts and chemical shift anisotropies, were obtained for 30 dialkyldithiophosphate compounds: (i) initial potassium salts, (ii) mononuclear nickel-(II), (iii) binuclear zinc(II), (iv) polymeric zinc(II) diethyl, and (v) tetranuclear zinc(II) complexes. The chemical shift anisotropy parameters δ_{aniso} and η were estimated from the spinning sideband patterns using an earlier developed simulation program in the Mathematica front end,[5] and thereafter, the principal values of the ^{31}P CST, δ_{11}, δ_{22}, and δ_{33}, were calculated. It was found that the chemical shift anisotropy of nickel(II) and zinc(II) dialkyldithiophosphate complexes varies considerably between terminal and bridging types of ligands in these molecular systems. There is a distinct correlation between the S−P−S bond angle in the compounds (ii), (iii), (iv), and (v) and the values of the principal component δ_{22} of the ^{31}P chemical shift tensor: δ_{22} increases almost linearly as the S−P−S bond angle increases, while the other two principal components, δ_{11} and δ_{33}, are almost conserved.

Ab initio quantum mechanical calculations show the same trend between σ_{22} and the S−P−S bond angle, both in the model $[(CH_3O)_2PS_2]^-$ fragment and in the nickel(II) and zinc(II) dialkyldithiophosphate complexes with known single-crystal X-ray diffraction structures. σ_{22} decreases from 218 to 126 ppm as the bond angle increases from 93° to 125°. For the O−P−O angle in the range between 87.4° and 108.6°, σ_{22} varies by ca. 25% and shows a minimum at 96°. The calculations also showed a small variation of the σ_{11} and σ_{33} principal components on both O−P−O and S−P−S bond angles. Ab initio calculations also revealed substantial variations in σ_{11} and σ_{22} principal values as functions of P−O and P−S bond lengths in the ranges 1.61−1.71 and 1.95−2.05 Å, respectively. However, considering the small range of bond lengths present in the crystal structures of the dialkyldithiophosphate complexes in this study, for these parameters, it was impossible to elucidate any correlation between experimental and calculated principal values of the ^{31}P chemical shift tensors. However, it seems that most of predictions from ab initio calculations of ^{31}P chemical shifts and chemical shift anisotropies in dialkyldithiophosphate compounds are qualitatively and, to a certain extent, quantitatively reliable.

The deviations in the tensor components due to the distortion of the $[(CH_3O)_2PS_2]^-$ fragment upon bonding of a metal ion (Zn or Ni) are reasonably small for the terminal ligands. The deviations for the bridging ligands, however, are too large to be relied upon. The higher flexibility of the eight-membered ring structure in the bridging part of the molecule probably causes larger distortions of the geometry and, therefore, also in the symmetry of the electronic environment around the ^{31}P sites, in comparison to the more rigid four-membered ring in the terminal parts of the molecule. Similar to ^{13}C CST correlation experiments in peptides and proteins,[23] in principle, different types of experiments correlating ^{31}P CSTs of the terminal type of ligands can be designed for estimation of certain torsion angles and other structural features in dialkyldithiophosphates and similar compounds in powder samples.

Acknowledgment. We are grateful to CHEMINOVA AGRO A/S for the dialkyldithiophosphate chemicals, which were kindly supplied for this study. The CMX-360 spectrometer was purchased with a grant from the Swedish Council for Planning and Coordination of Research (FRN). We thank the foundation to the memory of J. C. and Seth M. Kempe for a grant from which part of the NMR equipment has been purchased. A part of this work was financed by Agricola Research Centre at Luleå University of Technology. A.C.D. acknowledges support from the National Science Foundation under Grant No. CHE-9874424. Acknowledgment is made to the donors of the Petroleum Research Fund, administered by the American Chemical Society, for partial support of this research. We thank Dr. Douglas Baxter, the Division of Chemistry, Luleå University of Technology, for fruitful discussions.

Supporting Information Available: Definitions for the CSA parameters, details of CSA simulations and calculations of statistical errors; powder ^{31}P CP/MAS NMR spectra of potassium salts of *O*,*O*′-diethyl-, *O*,*O*′-di-isopropyl-, *O*,*O*′-di-isobutyl-, and *O*,*O*′-di-isoamyldithiophosphates (Figure 1S), mono-

nuclear nickel(II) dialkyldithiophosphate complexes (Figure 2S), polynuclear and binuclear zinc(II) dialkyldithiophosphate complexes (Figure 3S), and tetranuclear zinc(II) dialkyldithiophosphate complexes (alkyl = ethyl, *n*-propyl, isopropyl, and *n*-butyl; Figure 4S); ^{31}P static NMR spectra of powder *O*,*O*′-diethyldithiophosphate potassium salt and nickel(II) and zinc(II) complexes and tetranuclear $[Zn_4O\{S_2P(OC_3H_7)_2\}_6]$ complex (Figure 5S). This material is available free of charge via the Internet at http://pubs.acs.org.

JA0306112